

## Electronic Supplementary Information for

### Amorphous-amorphous transition in a porous coordination polymer

Hiroyoshi Ohtsu,<sup>a\*</sup> Thomas D. Bennett,<sup>b</sup> Tatsuhiro Kojima,<sup>c</sup> David A. Keen,<sup>d,e</sup> Yasuhiro Niwa,<sup>f</sup> and Masaki Kawano<sup>a\*</sup>

*a. Department of Chemistry, Graduate School of Science, Tokyo Institute of Technology, 2-12-1 Ookayama, Meguro-ku, Tokyo, 152-8550, Japan*

*b. Department of Materials Science and Metallurgy, University of Cambridge, 27 Charles Babbage Road, Cambridge CB3 0FS, United Kingdom*

*c. Department of Chemistry, Graduate School of Science, Osaka University, Toyonaka, Osaka, 560-0043*

*d. ISIS Facility, Rutherford Appleton Laboratory, Harwell Campus, Didcot, Oxfordshire OX11 0QX, United Kingdom*

*e. Department of Physics, Oxford University, Clarendon Laboratory, Parks Road, Oxford OX1 3PU, United Kingdom*

*f. Photon Factory, Institute of Materials Structure Science, High Energy Accelerator Research Organization (KEK), Tsukuba, Ibaraki 305-0801, Japan*

\* To whom correspondence should be addressed.

E-mail: mkawano@chem.titech.ac.jp (MK), ohtsu@chem.titech.ac.jp (HO)

| <b>Contents</b>   | <b>pages</b> |
|---|--------------|
| <b>Experimental Details</b>   | 3-4          |
| <b>Fig. S1 Structure of phase 1 (without solvent)</b>               | 5            |
| <b>Fig. S2 Structure of phase 4</b>                                 | 5            |
| <b>Fig. S3 TG-DSC of amorphous phase 1</b>                          | 6            |
| <b>Fig. S4 XRPD change of phase 2 after soaking to nitrobenzene</b> | 6            |
| <b>Fig. S5 XRPD of phase 2 and phase 3</b>                          | 7            |
| <b>Fig. S6 Optical images of phase 2 and phase 3</b>                | 7            |
| <b>Fig. S7 TG-DSC of amorphous phase 2</b>                          | 8            |
| <b>Fig. S8 Total scattering of each phase</b>                       | 9            |
| <b>Fig. S9 UV-Vis. spectra of each phase</b>                        | 10           |
| <b>Details of XAFS analysis</b>                                     | 11           |

## Experimental Details

### Materials

TPT<sup>11</sup> and network  $[(\text{ZnI}_2)_3(\text{TPT})_2(\text{C}_6\text{H}_5\text{NO}_2)_{5.5}]_n$  (phase **1**)<sup>10</sup> were prepared according to the method described in the literature. All other chemicals and reagents were used as received.

### Methods

*In-situ* powder X-ray diffraction data were collected at SPring-8 BL02B2 (Japan). Powder X-ray diffraction data were collected on a Bruker D8 ADVANCE instrument in-house using reflection mode. IR spectra were recorded on a Varian 670-IR FT-IR spectrometer by the ATR method. UV/vis/NIR spectra were recorded on a Shimadzu UV/Vis-NIR scanning spectrophotometer UV-3600 using the diffuse-reflectance method. Thermogravimetric (TG) analysis was carried out at a ramp rate of 5 K/min in a nitrogen flow (30 ml/min. or 50 ml/min.) with a Setaram Labsys Evo instrument. Elemental analyses were performed on an Elementar vario MICRO cube at Technical Support Center in Pohang University of Science and Technology.

### Isolation of Amorphous Phase 2

688.7 mg of white crystalline powder of phase **1**,  $[(\text{ZnI}_2)_3(\text{TPT})_2(\text{C}_6\text{H}_5\text{NO}_2)_{5.5}]_n$ , was heated at 483 K for 1.5 h. 360.1 mg of the yellow powder of phase **2** was collected with 74.7 % yield.

Elemental analysis:

Anal Calcd. for  $\text{C}_{36}\text{H}_{26}\text{I}_6\text{N}_{12}\text{Zn}_3$   $[(\text{ZnI}_2)_3(\text{TPT})_2(\text{H}_2\text{O})]$ : C, 27.02; H, 1.64; N, 10.50.

Found: C, 27.09; H, 1.64; N, 10.50

### Isolation of Amorphous Phase 3

25 mg of phase **2** was heated in TG-DSC machine (Setaram Labsys Evo) with ramp ratio of 5 K/min. The heating was stopped at 581 K and cooled down quickly and collected the sample.

Elemental analysis:

Anal Calcd. for  $\text{C}_{36}\text{H}_{28}\text{I}_6\text{N}_{12}\text{Zn}_3$   $[(\text{ZnI}_2)_3(\text{TPT})_2(\text{H}_2\text{O})_2]$ : C, 26.72; H, 1.74; N, 10.39.

Found: C, 26.85; H, 1.76; N, 10.36

### **XAFS measurements**

The powder sample of each phase (phase **1**, phase **2**, and phase **4**) was put between aluminum tape and sealed, following by hand-pressing to ensure uniformity of the powder. A mortar and pestle could not be used due to the sensitivity of samples to mechanical grinding. The aluminum tape with the powder sample of each phase was placed in a cell with the polyethylene windows. The XAFS spectra of Zn *K*-edge were recorded at 20 K and room temperature for all samples using the BL-12C or BL-9A stations at the Photon Factory in KEK, equipped with an Rh-coated collimation mirror, an Si(111) double-crystal monochromator, an Rh-coated focusing mirror and an Ni-coated double-mirror system for the removal of higher-order reflections.

The transmittance measurements for Zn *K*-edge were performed using the ionization chambers with the lengths of 17 and 30 cm to measure the incident and transmitted X-ray intensities ( $I_0$  and  $I$ , respectively) for samples. Nitrogen gas and an N<sub>2</sub>+Ar gas mixture were flowed in the ionization chamber for the  $I_0$  and  $I$  measurements, respectively. The content of Ar in the gas mixture was 50%.

### **PDF measurements**

X-ray total scattering data were collected at room temperature on each phase, using a PANalytical Ag-source X'pert Pro MPD lab diffractometer ( $\lambda = 0.561 \text{ \AA}$ ). Data collection was carried out using loaded 1.0 mm diameter quartz glass capillaries and collection times of approximately 18 h. Corrections for background, multiple scattering, container scattering, and absorption were applied using the GudrunX program.\*<sup>18,19</sup>

\*) Soper, A. K. Gudrun N and Gudrun X: Programs for Correcting Raw Neutron and X-Ray Diffraction Data to Differential Scattering Cross Section; Rutherford Applied Laboratory Technical Report RAL-TR- 2011-013; Science and Technology Facilities Council: Harwell, U.K.,2011.

**Structure of phase 1 (without solvent),  $[(\text{ZnI}_2)_3(\text{TPT})_2]_n$**

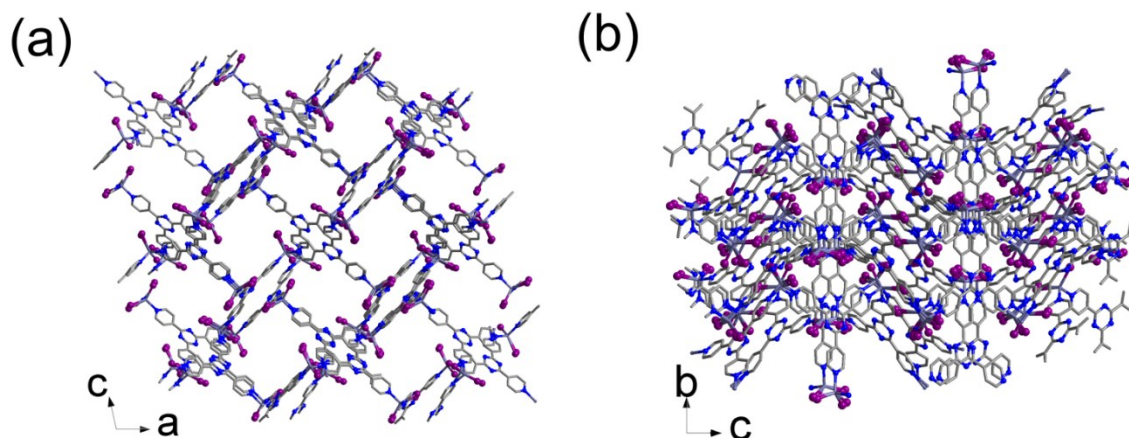


**Fig. S1** Crystal structure of phase 1,  $[(\text{ZnI}_2)_3(\text{TPT})_2]_n$  without solvent, (a) the  $b$ -axis projection, (b) the  $c$ -axis projection, Colors: Zn, light-purple; I, purple; C, grey; N, blue. Hydrogen atoms are omitted for clarity.

**Structure of phase 4,  $[(\text{ZnI}_2)_3(\text{TPT})_2]_n$**

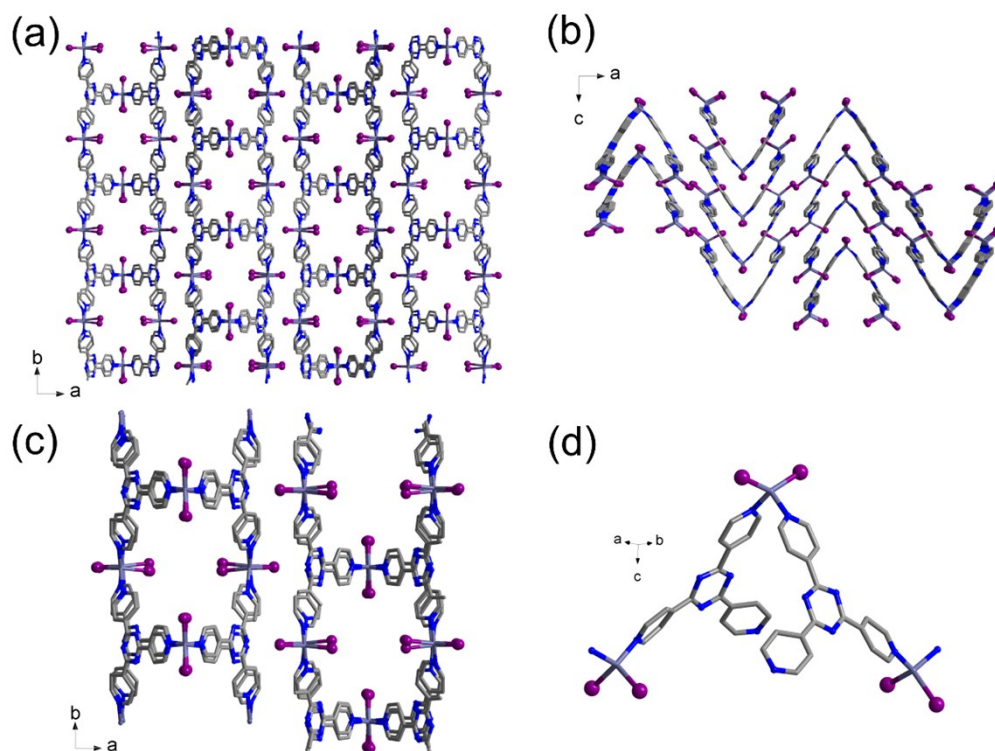


**Fig. S2** Crystal structure of phase 4,  $[(\text{ZnI}_2)_3(\text{TPT})_2]_n$ , (a) the  $c$ -axis projection, (b) the  $b$ -axis projection, (c) pore view from  $c$ -axis, (d) view of one saddle type unit, Colors: Zn, light-purple; I, purple; C, grey; N, blue. Hydrogen atoms are omitted for clarity.

### TG-DSC of amorphous phase 1

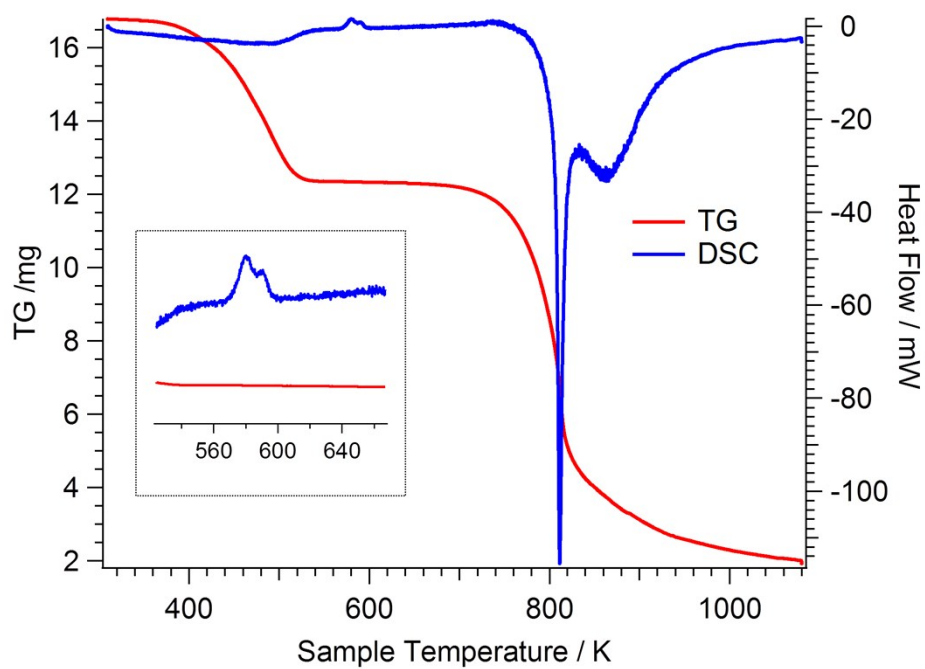


**Fig. S3** TG (red) and DSC (blue) of phase 1 (ramp rate: 5 K/min). Inset shows a magnified Figure.

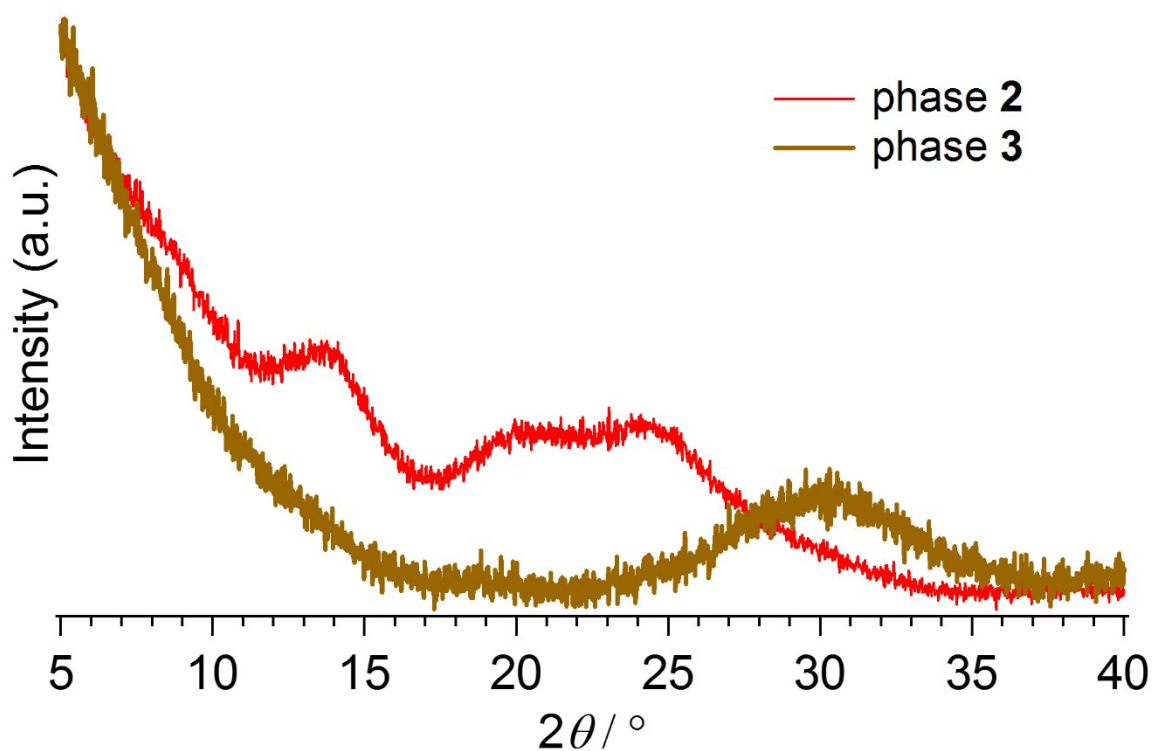


**Fig. S4** XRPD of phase 2 and phase 3.

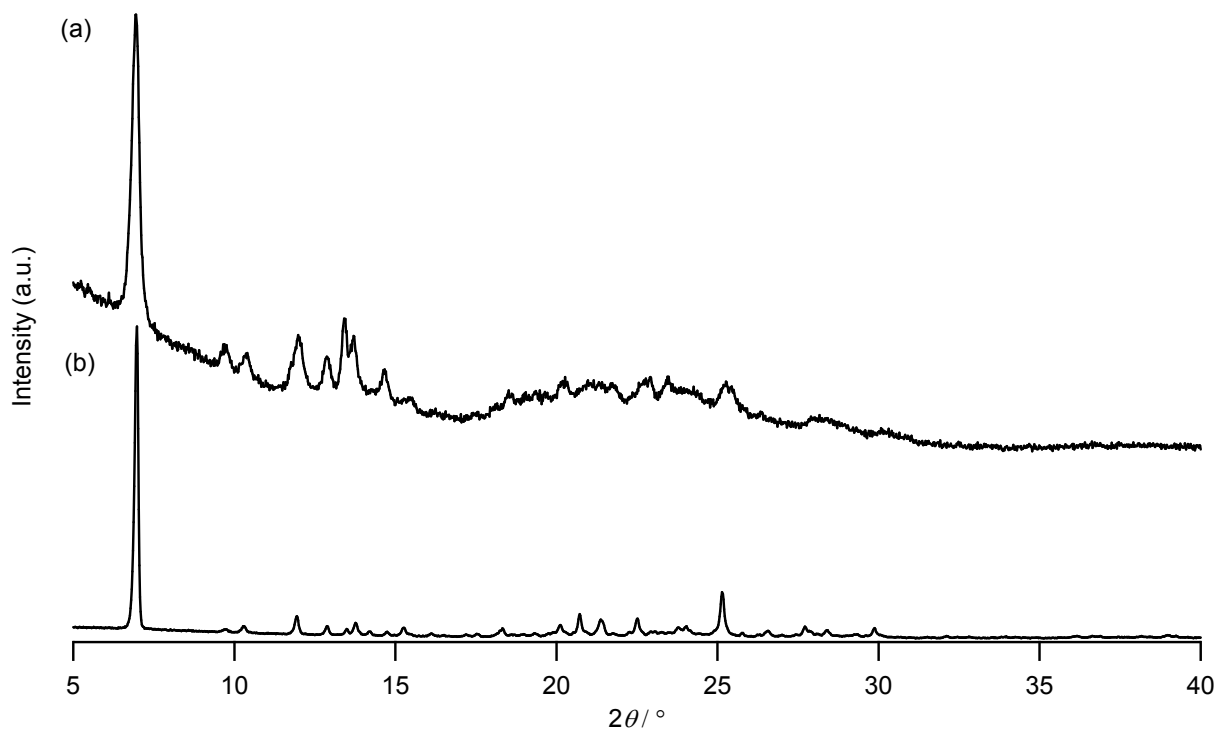


**Fig. S5** XRPD of (a) phase **2** after soaking to nitrobenzene and (b) simulated XRPD pattern of phase **1** from single crystal data. It reveals that phase **2** reversed back to phase **1** by immersion in nitrobenzene.

### Optical images of phase **2** and phase **3**



**Fig. S6** Appearance of amorphous phase **2** (left) and phase **3** (right).

## TG-DSC of amorphous phase 2

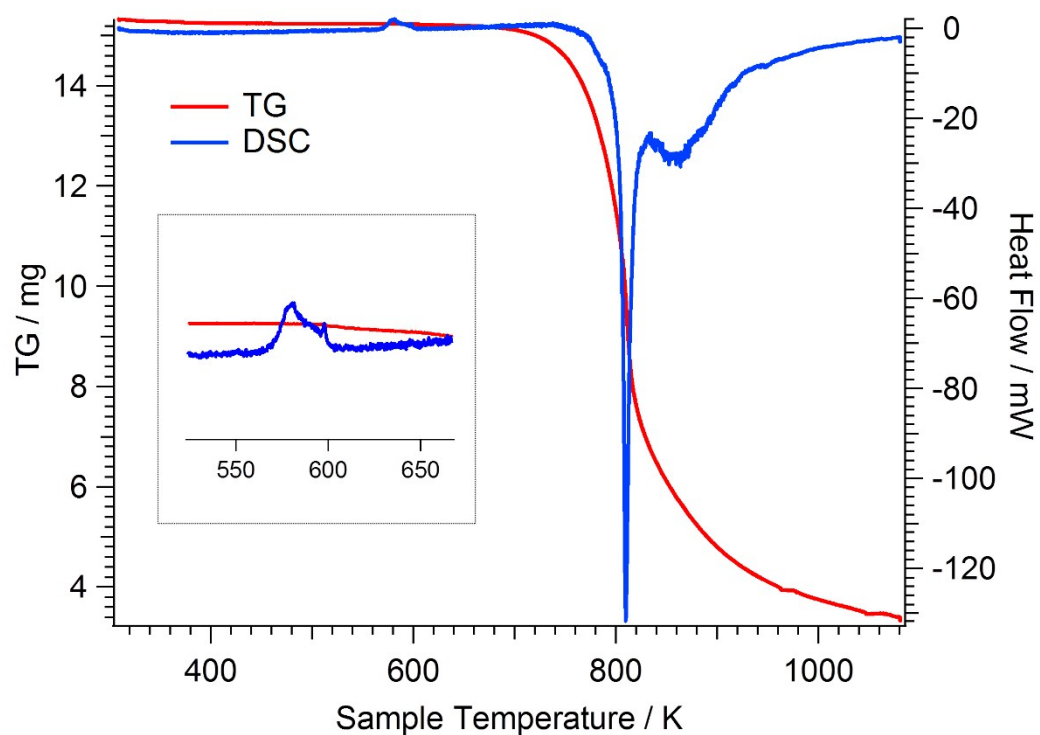


**Fig. S7** TG (red) and DSC (blue) of the amorphous phase 2 (ramp ratio: 5 K/min). Inset shows a magnified Figure.



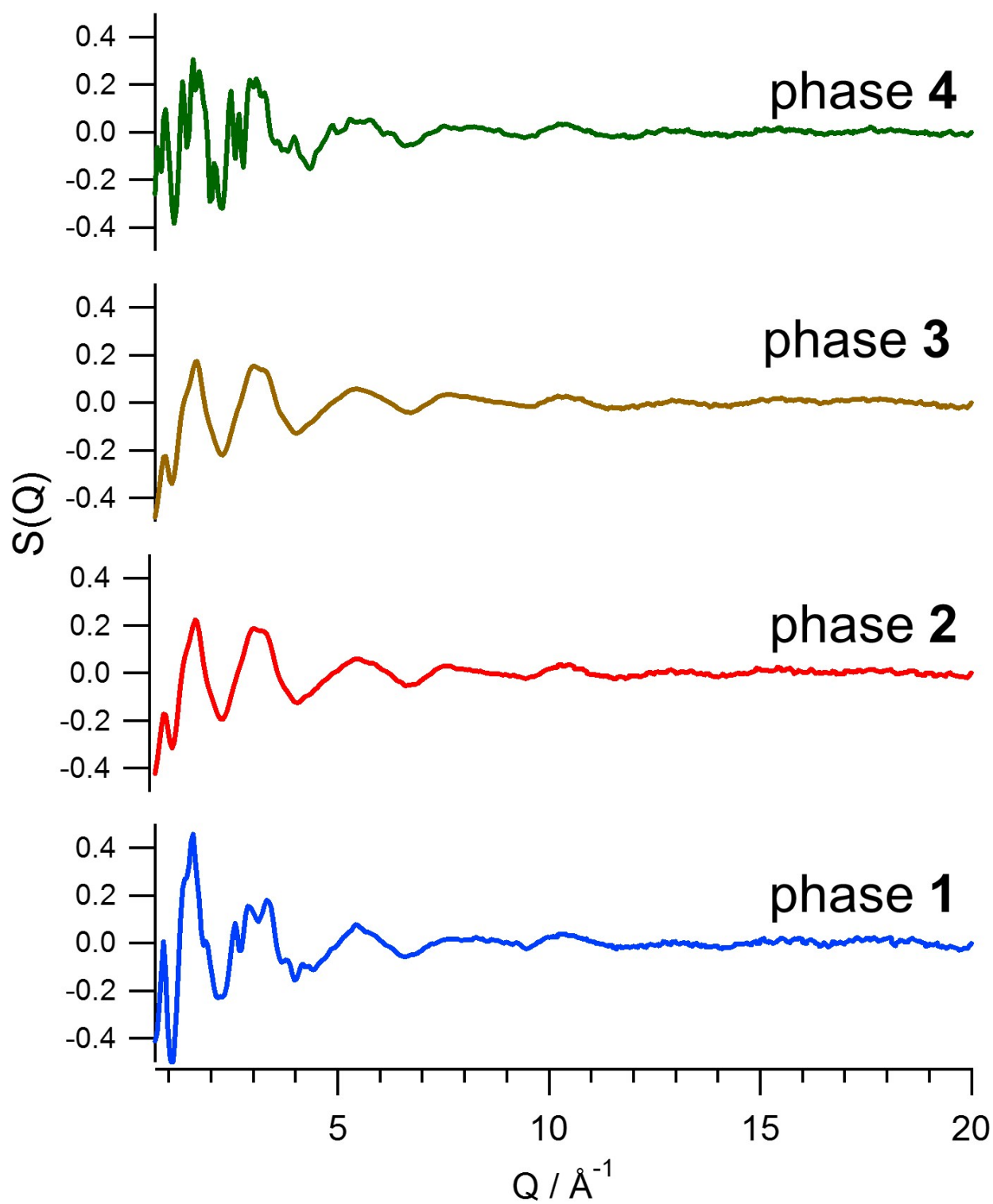


**Fig. S8** Total scattering,  $S(Q)$ , of each phase.

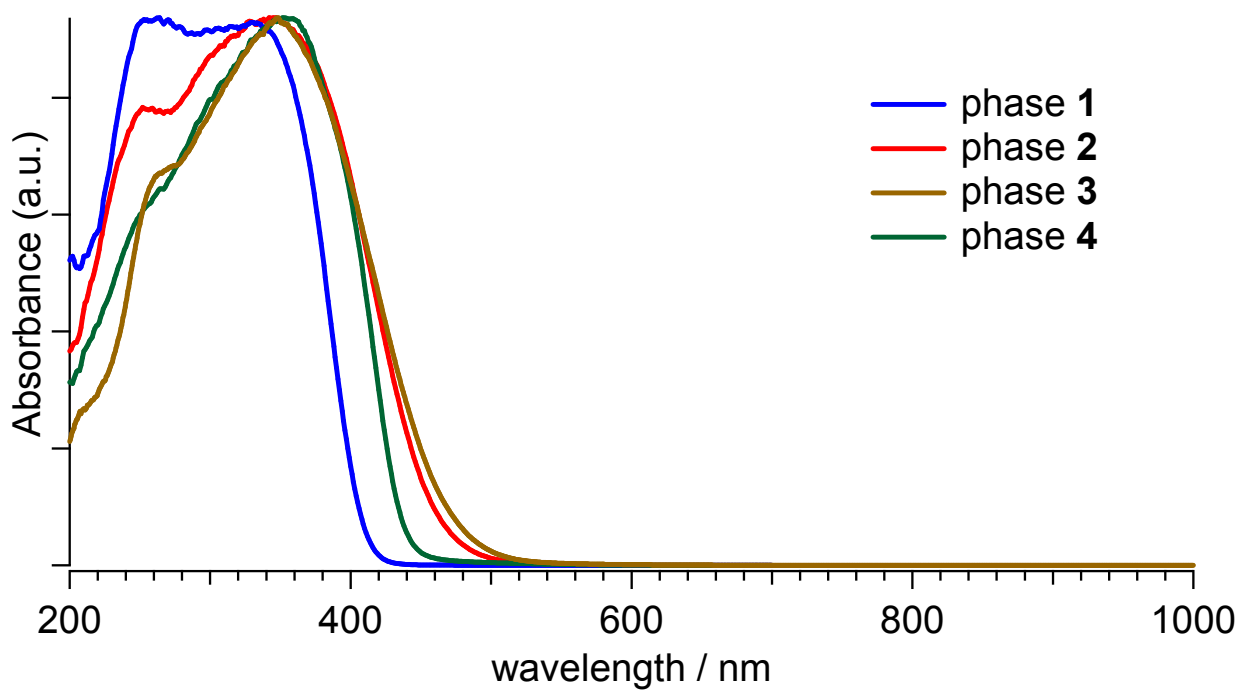


**Fig. S9** Diffuse-reflectance UV-Vis spectra of each phase. Absorbance were calculated by Kubelka-Munk transformation and normalized.

## Details of XAFS analysis of phase 2

The analysis of XAFS spectra of phase 2 was performed using IFEFFIT (using software Artemis). The structural parameters were determined by a curve fitting procedure in  $R$  space by using the FEFFIT program and ARTEMIS software packages as below.

XAFS measurements were carried out using ionization chambers with optimized detecting gases to measure the radiation intensity (incident intensity  $I_0$  and transmitted intensity  $I_t$ ) as mentioned above. The powder was dispersed onto the aluminum foil and the X-ray absorption was measured. The absorption spectra were calculated by  $\ln(I_0(E)/I(E))$ , where  $I(E)$  and  $I_0(E)$  are transmitted and incident X-ray intensity of energy ( $E$ ). The spectra were calibrated, averaged, pre-edge background subtracted, and post-edge normalized using standard procedures. The Fourier transformation of the  $k^3$ -weighted EXAFS oscillations,  $k^3 \chi(k)$ , from  $k$  space to  $r$  space was performed over a range of 2 – 11  $\text{\AA}^{-1}$  to obtain a radial structure function. The inversely Fourier-filtered data were analyzed by the usual curve-fitting method based on eq (1)

$$\chi(k) = \sum \frac{N_j S_0^2 f_j(k)}{k R_j^2} e^{-2k^2 \sigma_j^2} e^{-2R_j/\lambda(k)} \sin[2kR_j + \delta(k) + 2\phi_c(k)] \quad (1)$$

where  $f_j(k)$  is the backscattering amplitude from each of the  $N_j$  scatterers at distance  $R_j$  from the X-ray absorbing atom,  $\delta(k)$  is the central-atom phase shift,  $\sigma_j^2$  is the mean square fluctuation in  $R_j$ ,  $\lambda_j(k)$  is the mean free path of the photoelectron ejected, and  $S_0^2$  is the overall amplitude reduction factor. The values of  $f_j(k)$ ,  $\delta_j(k)$ , and  $\lambda_j(k)$  were estimated using the FEFF program by assuming the tetrahedral  $\text{ZnI}_2\text{py}_2$  structure, and the values for all possible scattering paths were considered in the fitting procedure including the multiple scatterings. The values of  $n_j$  and  $S_0^2$  was fixed to 1 to fix the coordination number of Zn,  $R_j$ , and  $\sigma_j^2$  were optimized by fitting Eq. (1) to the observed  $\chi(k)$  values using the FEFFIT program. This curve fitting procedure was performed in the  $R$  space by the Fourier transformation of both  $\chi(k)$  and  $\chi_{\text{cal}}(k)$  values in order to reduce the overestimation of the truncation error at the Fourier transformation.

The model of  $\text{ZnI}_2\text{py}_2$  (two iodine and two pyridine are coordinated to Zn tetrahedrally) was introduced to the fitting. The  $\text{ZnI}_2\text{py}_2$  model was introduced from the structure of phase 4. The fitting result is depicted in Fig. 3.

The fitting result of distance around Zn ion:

Zn-I : 2.551  $\text{\AA}$

Zn-N : 2.021, 2.100  $\text{\AA}$